Hindawi
Advances in Condensed Matter Physics
Volume 2023, Article ID 7366612, 11 pages
https://doi.org/10.1155/2023/7366612

Research Article

The Study on the Decolorization and Properties of Bismuth Glass

Sung-Hung Lan, Wei-Xiang Wang, Chien-Chon Chen, and Hsi-Wen Yang

Department of Materials Science and Engineering, National United University, 2, Lienda, Miaoli 360001, Taiwan

Correspondence should be addressed to Hsi-Wen Yang; hwyang@nuu.edu.tw

Received 28 March 2023; Revised 28 September 2023; Accepted 24 October 2023; Published 28 November 2023

Academic Editor: Raouf El Mallawany

PbO glass has an adverse effect on the environment; the bismuth glass has a high refractive index, low melting temperature, softening temperature, and glass transition temperature (T_g), so that it can be used as a lead-free glass, used in optoelectronics, electronics, optics, and other components, which bismuth glass has been proved to be an important replacement material. Due to the higher melting temperature, Bi^{3+} ions tend to partially reduce to the low valence state of Bi^0, which in turn causes coloration of the glass. In this experiment, the absorption peaks of glass oxidized brown color were observed at about 470 nm at 1,100°C ($Bi_2O_3 = 40$, 45 mol%) and 1,000°C ($Bi_2O_3 = 40$ mol%) for these three curves. The bismuth glass produced by high-temperature melting is not suitable for optical applications; by adding an oxidant (Sb_2O_3), which inhibits the reduction reaction of bismuth ions and maintains the ions in the state of Bi^{3+}, the glass becomes more transparent in appearance and the transmittance is also improved and raised to approximately 75%–80%, which proves that appropriate additives are sufficient to greatly improve the application of bismuth glass for optical components. In the research process, the density and molar volume were measured by Archimedes method, Raman analysis was used to explore the influence of its structural changes, UV/Vis spectroscopy was used to measure the transmittance and absorption spectra for analysis and discussion, and TMA was used to observe the thermal properties, in the hope of developing a good optical properties of the glass, and the present experiments have confirmed that the addition of a small amount of Sb_2O_3 changes the color of the glass from black to a light yellow, which can be better used in the optical glass.

1. Introduction

Adding PbO to glass can make the glass have good transmittance, stable structure, low-temperature glass characteristics, excellent optical properties, thermal properties, and electrical properties [1], but it easily causes harmful effects on the environment and the human body, and because the European Union has announced that it will not accept lead-containing products to enter into Europe, which limits the space for the development of lead-containing glass, therefore, the development of lead-free glass to replace leaded glass is the main research direction at present. In recent decades, phosphor–boron glasses have been extensively studied for their various technical applications, and such materials have better chemical durability due to the BO_4 unit-induced phosphoric acid chain network structure [2]. Compared with borate and silicate glasses, phosphate glasses have various advantages; in particular, the low melting temperature, low glass transition temperature (T_g), low glass softening temperature (T_s), high coefficient of thermal expansion (CTE), and high UV transmittance have led to a wide range of applications, especially as glass seals, fast ionic conductors and nonlinear optics, antimicrobials, implant surface treatments, optical amplifiers, and more [3, 4]. The basic structural unit of phosphate glass is PO_4 tetrahedron containing bridging oxygen (BO) atoms (BO) and nonbridging oxygen (NBO) atoms, which can form various phosphate anions by bonding with covalent BO atoms and classified in terms of Q^i, where i represents the number of BOs per (PO_4) tetrahedron, Q^0 units represent orthophosphate $(PO_4)^{3-}$ and Q^1 units represent pyrophosphate $(PO_3)^{2-}$, in superphosphate glasses, three BO atoms are shared between the tetrahedra, thus forming a 3D cross-linked phosphate network [5]. Moreover, this phosphate glass ceramic is also an electronic conductor, but this material has the disadvantage of high dielectric loss. Haily et al. [6] replaced TiO_2 with Bi_2O_3 and developed a new glass composition $10Bi_2O_3$–10BaO–$80P_2O_5$ in the BaO–Bi_2O_3–P_2O_5 system with higher dielectric properties than titanium-containing glasses. Phosphate glass has two basic drawbacks: high moisture absorption and low chemical durability. To overcome these problems, many scientists have added additives to phosphate precursors [7]. Bismuth oxide (Bi_2O_3), whose Bi^{3+} properties are similar to Pb^{2+} of lead oxide (PbO), both have the same electronic configuration, as well as high polarizability, and the glass also has a low melting temperature, high density, high refractive index and other characteristics, which can be used to replace the lead oxide to develop a variety of lead-free glass products [8]; therefore, bismuth glass is one of the most promising glasses without considering leaded glass [9, 10]. However, as the melting temperature rises and the bismuth content increases, it is easy to cause the glass color to change from light yellow to dark brown or even black, and this coloring defect is not conducive to the application of optical glass. Zhang et al. [11] investigated the effect of Sb_2O_3 addition on the Bi_2O_3–B_2O_3–SiO_2 glass system, and the glass samples were melted at 1,100°C–1,200°C. From the results of UV/Vis spectroscopy, with the addition of Sb_2O_3, the cutoff wavelength is shifted to longer wavelengths, and this phenomenon is reflected in the electronegativity of Bi–O bonding. It is known that the bismuth ions in the high valence state are more electronegative than the bismuth ions in the low valence state and that the oxygen ions are more likely to be delinked from the cation bond; in other words, the oxidation effect brought by the addition of Sb_2O_3 keeps the Bi ions in the high valence state, inhibits the reduction of Bi^{3+} into Bi^0, and at the same time, it also makes the glass appearance lighter in color, and there is an obvious upward trend in the overall transmittance of the glass. In this study, the glass composition (B_2O_3–ZnO–Bi_2O_3–P_2O_5) will be the main research, and investigate the color change of glass by changing the content of Bi_2O_3, the temperature of the process, and the addition of Sb_2O_3 redox additives that can make the glass lose its color, in the hope that the degree of reduction of Bi_2O_3 can be controlled by these factors. Because the bismuth glass produced by high-temperature melting is not suitable for optical applications, and there are only a few literatures exploring how to eliminate the coloring phenomenon, and the ultimate goal of this study is to solve the coloring problem by decolorization effect, and it is found that by adding a small amount of Sb_2O_3, the color of the glass is changed from black to light yellow. In the process of research, the density and Mohr volume were measured by Archimedes method, the effect of structural changes was investigated by Raman analysis, the transmittance and absorption spectra were analyzed and discussed by UV/Vis, and the thermal properties were observed by TMA, which proved that the decolorization effect had a significant result, and the glass with good optical properties was developed for better application in optical glass.

2. Materials and Methods

Results of two experiments: (1) the study of bismuth zinc borophosphate glass properties, structure, and application and (2) the influence of Bi_2O_3 content and melting temperature on the structure and properties of Bi_2O_3–ZnO–B_2O_3 glasses [12, 13]; therefore, the present study was carried out by the process of (80–x) B_2O_3–$x$$Bi_2O_3$–$10P_2O_5$–10ZnO ($x = 30, 35, 40, 45$ mol%) plus Sb_2O_3 (3 mol%). Baker, 99.7%), Bi_2O_3 (Sigma-Aldrich, 98%), $(NH_4)H_2PO_4$ (Scharlau, 98%), Sb_2O_3 (Alfa Aesar, 99.6%), where $10P_2O_5$–10ZnO is a fixed component, which is melted at 900, 1,000, and 1,100°C process temperature, respectively. In the experiment, the weight of the required raw material powder was calculated according to the mole fraction of the composition. The configured raw materials are mixed uniformly by dry ball milling and then put into the alumina crucible, which is heated up to 450°C in a high-temperature furnace at a rate of 10°C/min, and the temperature is held for 1 hr to remove the moisture in the raw material powder and make $(NH_4)H_2PO_4$ fully reacted to P_2O_5, then raise the temperature to different process temperature, hold the temperature for 1 hr to make it clarified to promote the homogeneous mixing of the glass paste, and then take out the molten glass liquid from the high-temperature furnace, and cast it onto the carbon plate preheated to annealing temperature for molding. In order to eliminate the thermal stress caused by the rapid cooling of the glass, the glass is sent to an annealing furnace at 450°C for 2 hr and then slowly cooled to room temperature in the furnace to complete the preparation of the glass samples.

Raman spectroscopy was performed at room temperature, and the wave number range was measured from 0 to 1,600 cm^{-1}. During the process, a Microscopic Conjugated Focus Raman/Fluorescence Spectroscopy System (UniDRON) was used.

The annealed glass specimens were cut into $20 \times 15 \times 2$ mm sizes and ground and polished; the spectrophotometer (Shimadzu UV-2401PC spectrophotometer, Japan) was used to measure the wavelength range from 200 to 900 nm for UV–Vis spectral transmission analysis.

The glass samples were ground into square specimens of $5 \times 5 \times 5$ mm with the top and bottom parallel, and the glass transition temperature (T_g), glass softening temperature (T_d), and CTE (α) of 200–300°C in the working area was measured by using a thermomechanical analyzer (Perkin Elmer TMA 7, USA) with a heating rate of 10°C/min at room temperature, and the heating was continued until the glass appeared to be softened.

The density (D) of the glass was measured by cutting the glass block into appropriate-sized specimens, using Archimedes' principle and pure water as the impregnating liquid, and measuring $D = W_d/(W_d - W_s)$ at room temperature, where D is the density, W_d is the dry weight of the sample, and W_s is the suspended weight of the sample. Molar volume $V_M = \sum \frac{x_i M_i}{D}$, where x_i is the molar fraction of each constituent oxide, M_i is the molecular weight of each constituent oxide, and D is the density of the glass measured by Archimedes' method.

Table 1: Characteristics of Raman vibration peaks and bands.

Wavenumber (cm^{-1})	Vibrational mode	Reference
100–200	Symmetric stretching vibration of Bi–O–Bi in (BiO_3) and (BiO_6) units	[14–16]
200–550	Symmetric stretching vibration of the Bi–O–Bi bond in the (BiO_6) unit	[15–17]
570–620	Stretching vibration of Bi–O^- in (BiO_6) unit	[14–16]
700–740	B–O–B bending vibration of (BO_3) structural unit	[16, 18, 19]
950–1,000	Symmetric stretching vibration of B–O^- in (BO_3) unit	[16, 20–23]
1,220–1,500	Asymmetric stretching vibration of B–O^- in (BO_3) and (BO_4) units	[19, 24, 25]

3. Results and Discussion

3.1. Raman Structure Analysis. The glass structure is mainly measured and analyzed by the Raman spectrum to observe the changes of various basic bonding modes in the glass structure when the composition of the glass and the temperature of the process are changed. The characteristic peaks and bands corresponding to the results of Raman analysis are organized as shown in Table 1.

According to the literature [2, 26], Raman spectra caused by heavy metal oxides, such as Bi_2O_3, can be categorized into four major groups of characteristic peaks: (1) low wavelength Vibrations (less than 100 cm^{-1}) caused by the Raman effect; (2) vibrations induced by heavy metal ions (70–160 cm^{-1}); (3) vibrations induced by BOs (300–600 cm^{-1}); and (4) vibrations induced by NBOs (>600 cm^{-1}).

From the experimental results, the Raman spectra of B_2O_3–Bi_2O_3–P_2O_5–ZnO series glasses were analyzed in the range of wave numbers from 0 to 1,500 cm^{-1}, it was found that the glass system could be classified into seven Raman scattering peaks, which were mainly located at the wave numbers of about 135, 270, 400, 570, 710, 1,000, and 1,200 cm^{-1}.

It was found that among all the peaks, (135, 400 cm^{-1}), (570 cm^{-1}), and (1,000 cm^{-1}) were the most obvious:

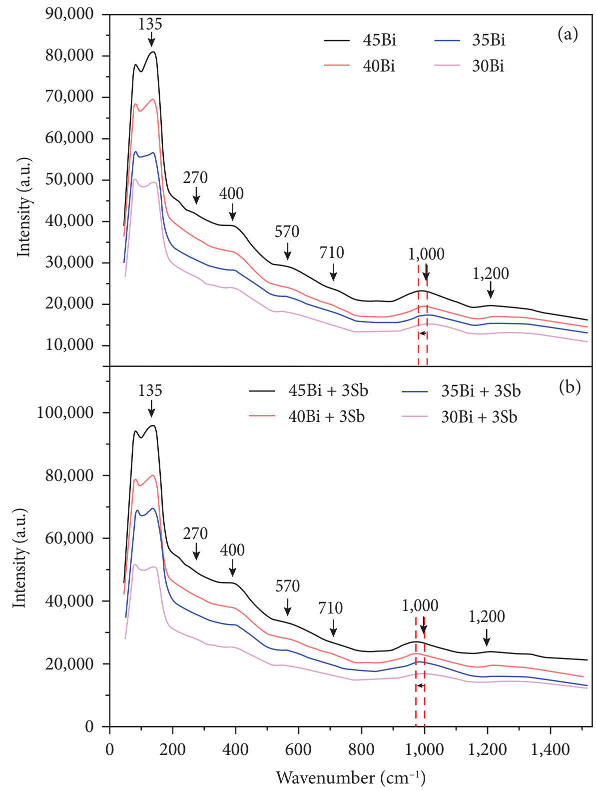

Figure 1: Raman spectra of a series of glasses melted at 1,000°C: (a) $(80-x)B_2O_3$–xBi_2O_3–$10P_2O_5$–10ZnO; (b) $(80-x)B_2O_3$–xBi_2O_3–$10P_2O_5$–$10ZnO + 3Sb_2O_3$.

(1) The characteristic peaks at 135 and 400 cm^{-1} [14, 15] are shown in Figures 1 and 2; the intensity of the peaks increases with the increase of the content of Bi_2O_3 at the same temperature with or without the addition of Sb_2O_3; from Figures 3 and 4, at the same Bi_2O_3 content, with or without the addition of Sb_2O_3, the strength of this peak increases with the decrease of temperature, which indicates that the number of Bi–O–Bi bonding in the glass increases, and the Bi–O–Bi bonding is longer and weaker, thus leading to the decrease of the overall structural strength of the glass. This means that the number of Bi–O–Bi bonds in the glass increases, while the longer Bi–O–Bi bonds have weaker bonding energy, resulting in a decrease in the overall strength of the glass structure, which affects the glass transition temperature (T_g), the glass softening temperature (T_d) and the CTE of the glass structure, this phenomenon is also evidenced by the thermal analysis of the glass in Section 3.3.1. Further comparing the structural changes by adding Sb_2O_3, as shown in Figures 1 and 2, it can be found that no matter under 1,000 or 1,100°C, the changing trend of this peak of the glass with Sb_2O_3 is relatively smooth, which indicates that the structural changes are more stable.

(2) The characteristic peak at 570 cm^{-1} [14, 16, 24] is shown in Figures 1 and 2, which is slightly enhanced with the increase of Bi_2O_3 content at the same temperature with or without the addition of Sb_2O_3; from Figures 3 and 4, at the same content of Bi_2O_3, with or without the addition of Sb_2O_3, the intensity of this peak slightly increases with the decrease of temperature, which indicates an increase in the number of NBO in this glass structure, and corresponds to the result of the characteristic peak at 1,000 cm^{-1}, which leads to the generation of Bi–O–B bonds.

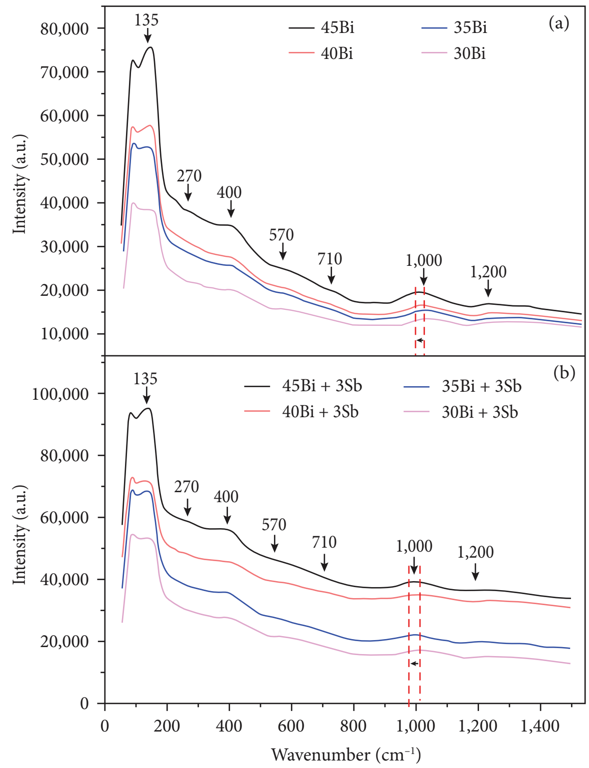

Figure 2: Raman spectra of a series of glasses melted at 1,100°C: (a) $(80-x)B_2O_3$–xBi_2O_3–$10P_2O_5$–$10ZnO$; (b) $(80-x)B_2O_3$–xBi_2O_3–$10P_2O_5$–$10ZnO + 3Sb_2O_3$.

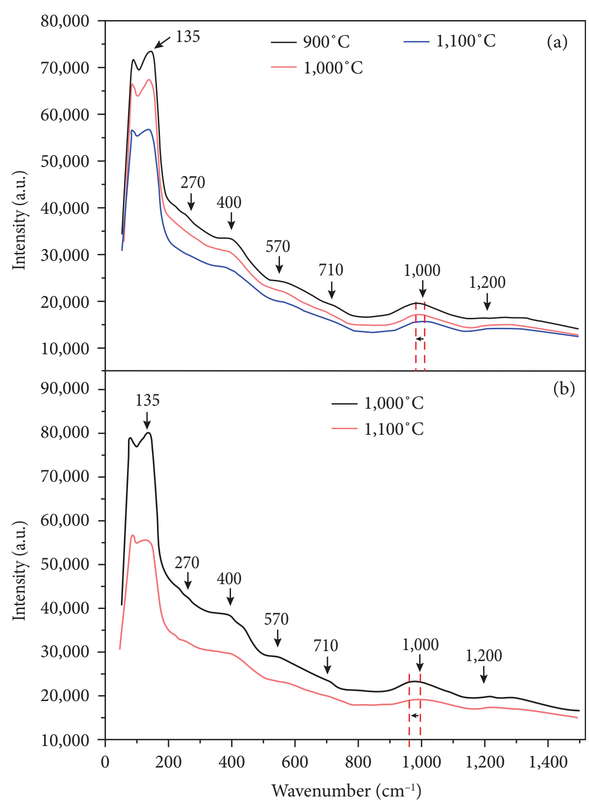

Figure 3: Raman spectra of a series of glasses melted at different temperatures: (a) $40B_2O_3$–$40Bi_2O_3$–$10P_2O_5$–$10ZnO$; (b) $40B_2O_3$–$40Bi_2O_3$–$10P_2O_5$–$10ZnO + 3Sb_2O_3$.

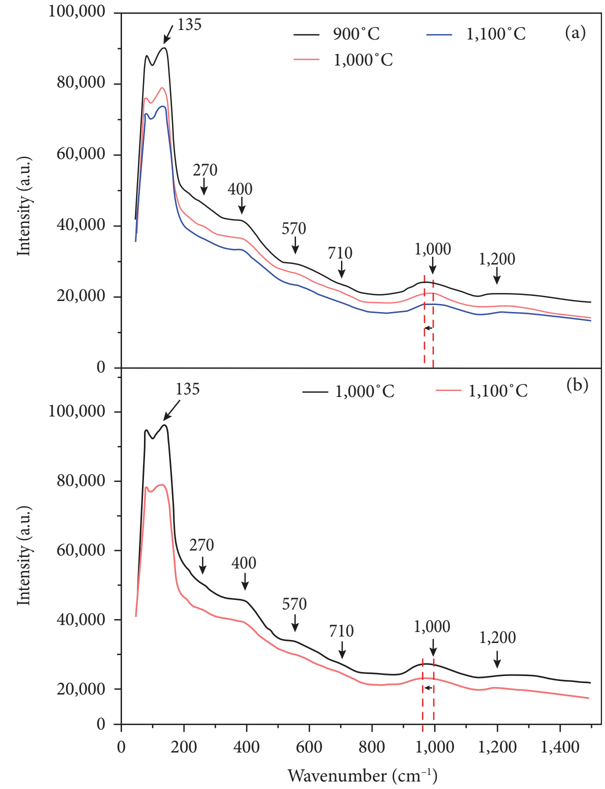

Figure 4: Raman spectra of a series of glasses melted at different temperatures: (a) $35B_2O_3$–$45Bi_2O_3$–$10P_2O_5$–$10ZnO$; (b) $35B_2O_3$–$45Bi_2O_3$–$10P_2O_5$–$10ZnO + 3Sb_2O_3$.

(3) The characteristic peak at 1,000 cm^{-1} [20–23] is shown in Figures 1 and 2, which is shifted to a lower wavelength with the increase of Bi_2O_3 content at the same temperature with or without the addition of Sb_2O_3; From Figures 3 and 4, it can be seen that at the same content of Bi_2O_3, with or without the addition of Sb_2O_3, the peak is shifted to a lower wavelength with the decrease of temperature. This phenomenon may be due to the high polarizability of Bi^{3+} ions, and at low temperatures, Bi^{3+} ions are not easily reduced to low valence ions. Therefore, when more Bi^{3+} ions enter into the structure of the boron–oxygen network, the density of the electron cloud around the O^{2-} in the B–O–B bond increases, which in turn induces the formation of the B–OB bond. For elastic stretching vibration, the strength of the stretching vibration of the BiO bond is lower than that of the BO bond, making the frequency of the Bi–O–B vibration smaller. In the glass system xBi_2O_3–$(20-x)K_2O$–$30TiO_2$–$50P_2O_5$ in the literature of Haily et al. [3], the increase in the number of oxygen atoms in the structure when Bi_2O_3 replaces K_2O promotes the structural units to be connected via coangle connections, and the interactions between Bi_2O_3 (BiO_6) and P_2O_5 (PO_4) form the P–O–Bi bonding, which leads to a decrease in the overall glass structure strength due to the shift of the absorption peak to lower wavelengths. The increase in the amount of NBO in this glass structure shifts the absorption peaks

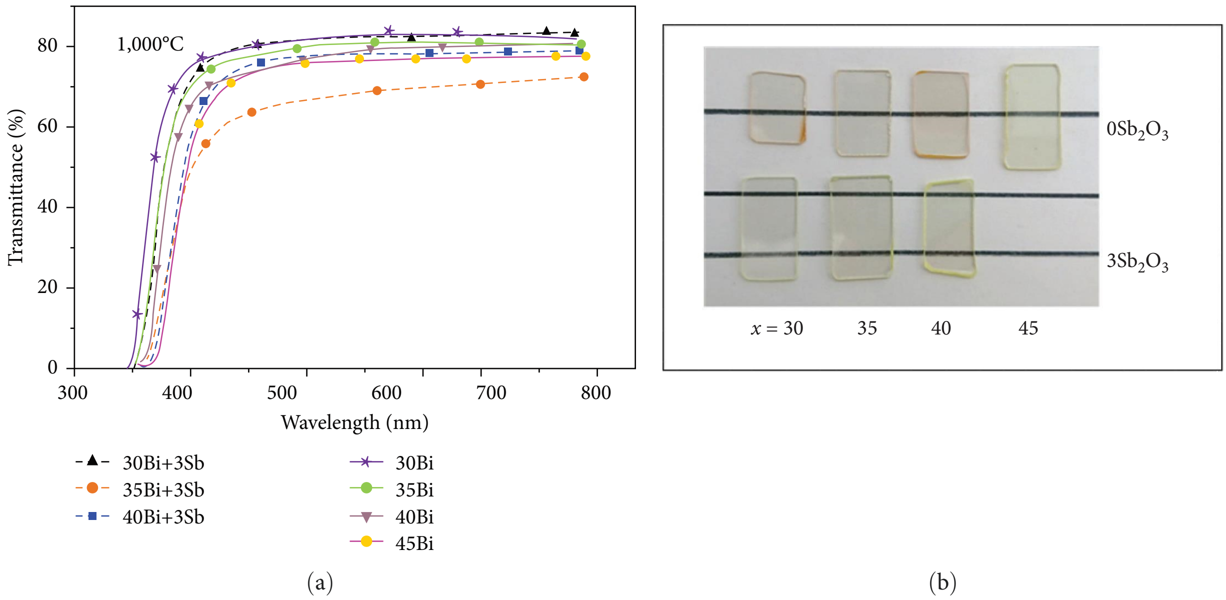

FIGURE 5: (a) The transmittance curves of $(80-x)B_2O_3$–xBi_2O_3–$10P_2O_5$–$10ZnO + (0, 3Sb_2O_3)$ melted at 1,000°C; (b) appearance of the glass samples for transmittance measurement.

to lower wavelengths, resulting in a decrease in the strength of the overall glass structure. The bonding strength affects the glass structure with a decrease in the glass transition temperature (T_g), glass softening temperature (T_d), and an increase in the CTE in accordance with the experimental results.

3.2. UV/Vis Absorption. The UV absorption of glass is generated by photon energy exciting the valence electrons of anions in the glass structure, causing them to jump from the ground state to the excited state [27]. For oxide glass, oxygen ions are fixed anions, and the UV cutoff wavelength of the glass is mainly determined by the characteristics of the chemical bonding between the oxygen ions and the cations. This characteristic is related to the radius size and coordination number of the cations. If the electronegativity of the cation is high, the electronegativity of the oxygen ions in the glass is also increased, and the electron excitation becomes difficult, causing the cutoff wavelength to shift to a shorter wavelength.

From a structural point of view, if the oxygen ions in the glass network structure are changed from the bridged state to the nonbridged state, the energy required to excite the electrons to migrate will be reduced because the nonbridged oxygen has excess electrons, and it is easier to excite the electrons in the nonbridged oxygen, resulting in the UV absorption limit moving to the long wavelengths; therefore, the addition of the network modifier in the glass can cause the UV absorption limit to shift to the visible light region. Figures 5 and 6 show the transmission curves of $(80-x)$ B_2O_3–xBi_2O_3–$10P_2O5$–$10ZnO + (0, 3Sb_2O_3)$ melted at 1,000 and 1,100°C. It can be observed from the graphs that the cutoff wavelength is shifted to the long wavelength as the content of Bi_2O_3 increases, and this phenomenon is due to the increase in the amount of NBO in the glass structure. From Raman analysis, as shown in Figures 1 and 2, the intensity of the characteristic peak of the NBO in the $[BiO_6]$ unit at the wavelength of $570\,cm^{-1}$ increases slightly with the increase of the content of Bi_2O_3, which indicates that the number of NBO in this glass structure increases, and it is easier to excite the electrons in the NBO due to the excess electrons in the NBO, which results in the shift of the cutoff wavelength to the longer wavelengths.

In addition, the degree of transmittance was also investigated, as shown in Figure 5. At 1,000°C, the degree of transmittance was in the range of 75%–80% with or without the addition of Sb_2O_3, and the degree of transparency was also good in appearance. In Figure 6, it can be observed that the glass without added Sb_2O_3 not only has a darker orange-brown color but also has a poorer transmittance. However, according to the literature [24], at higher melting temperatures, Bi^{3+} ions tend to partially reduce to the low-valent state of Bi^0, which results in the coloration of the glass, and the orange-brown coloration causes the glass to have an absorption peak in the contrasting wavelength band, i.e., around 470 nm in the figure. Therefore, by adding an oxidant (Sb_2O_3), the reduction reaction of bismuth ions is inhibited, and the ions are kept in the state of Bi^{3+}, thus improving the coloring problem. As shown in Figures 5(a) and 5(b), it can be observed that the appearance becomes more transparent, and the transmittance has improved and increased, remaining between 75%–80%.

Transmittance analyses were carried out to compare the Bi_2O_3 content of 40 and 45 mol% with the same composition and at different temperatures. From Figures 6(a) and 6(b), it can be found that the increase of Bi_2O_3 content decreases the overall transmittance of the glass, and it can be observed that the transmittance of the glass melted at 1,000°C is higher

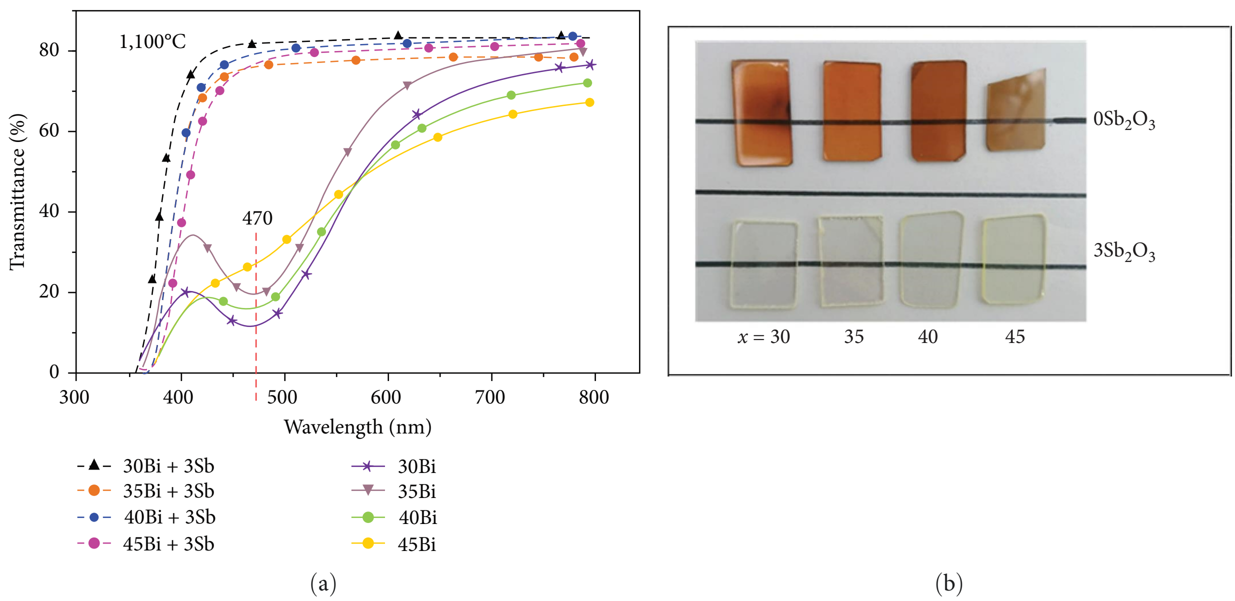

Figure 6: (a) Curves of the transmittance of $(80-x)B_2O_3$–xBi_2O_3–$10P_2O_5$–$10ZnO + (0, 3Sb_2O_3)$ glasses melted at 1,100°C; (b) appearance of the glass samples for transmittance measurement.

than that of the glass melted at 900°C, which may be due to the unevenness of the glass when it is melted in low temperature. Although the glass samples with Bi_2O_3 content of 40 and 45 mol% have a certain degree of transparency in appearance, there may be defects inside the glass that are not visible to the naked eye, which makes its transmittance relatively low. In the curve graphs, an absorption peak is observed at about 470 nm for the three curves at 1,100°C ($x = 40$, 45 mol%) and 1,000°C ($x = 40$ mol%), which are glassy orange-brown absorption peaks, which are similar to Haily et al. [28] literature (visible region) is characterized by a weak and broad absorption centered at 500 nm, which is attributed to the position of the absorption of the electronic transition of the ions.

From Figures 7(a) and 7(b), it can be found that the increase of Bi_2O_3 content decreases the overall transmittance of the glass, and it can be observed that the transmittance of the glass melted at 1,000°C is higher than that of the glass melted at 900°C. Figure 7(c) shows the appearance of the glass samples at 900°C; all the glasses, except for the ones with $x = 40$, 45 mol%, have inhomogeneities.

3.3. Thermal and Physical Properties of Glass

3.3.1. Thermal Properties of Glass. At the point where the thermal expansion curve of the glass turns into the transformation curve (the temperature at the intersection of the two tangent lines), that is, the transformation temperature (T_g) of the glass, and when the glass softens for a short period of time, there will be a peak, and the temperature at the top of the peak, that is, the softening temperature (T_d) of the glass.

Figures 8 and 9 show the results of the TMA experimental analysis of the B_2O_3–Bi_2O_3–P_2O_5–ZnO system composition glass, which contains the glass transition temperature (T_g), glass softening point (T_d), and CTE. Since T_g, T_d, and CTE are related to the bond strength and network density in the glass network, when the bond strength is stronger and the network density is larger, the molecular bond length is shorter, the glass transition temperature is higher, and the CTE is lower; on the contrary, if the bond strength is weaker and the network density is smaller, the molecular bond length is longer, the glass transition temperature is lower, and the CTE is higher.

From Figures 8 and 9, it can be observed that with the increase of Bi_2O_3 content, the glass transition temperature (T_g) and glass softening point (T_d) show a decreasing trend, while the CTE shows an increasing trend. This phenomenon can be seen from the results of Raman analysis as mentioned above. The characteristic peaks at 135 and 400 cm^{-1}, as shown in Figures 1 and 2. It shows that the strength of the peaks increases with the increase of the content of Bi_2O_3 at the same temperature, with or without the addition of Sb_2O_3, because the bonding energies of Bi–O–Bi and B–O–Bi are weaker than that of B–O–B. The peaks are also stronger than that of Bi–O–Bi, B–O–Bi, and the strength of this peak increases with the increase of Bi_2O_3 content. The increase in the content of Bi_2O_3 in place of B_2O_3 will lead to an increase in the number of Bi–O–Bi bonds, as well as the creation of B–O–Bi bonds, and at the same time, a decrease in the number of B–O–B bonds, thus leading to a decrease in the strength of the overall glass structure, which in turn leads to a decrease in T_g and T_d and an increase in CTE.

In addition, if we compare the situation with and without the addition of Sb_2O_3 at the same temperature, as shown in Figure 8(a), the glass is melted at 1,000°C ($+0Sb_2O_3$), and when the content of Bi_2O_3 rises, the T_g decreases from 494.7 to 463.2°C, and the T_d decreases from 537 to 496.2°C, as shown in Figure 8(b), the glass was melted at 1,000°C ($+3Sb_2O_3$), and when the content of Bi_2O_3 increased, the T_g decreased from 500.1 to 483.3°C, and the T_d decreased from 542.5 to 519.4°C. From the comparison of Figures 8(a)

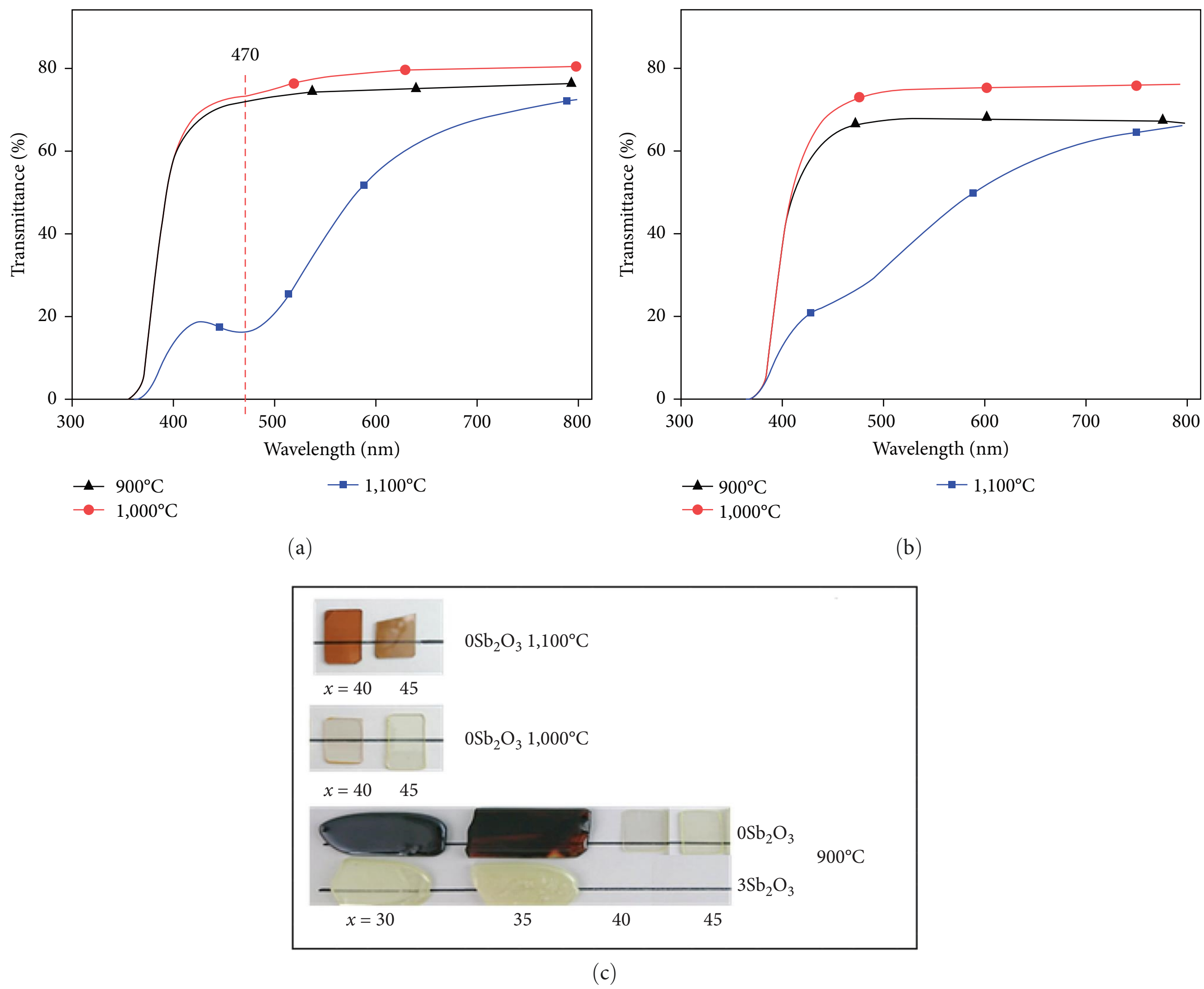

Figure 7: Curves of the transmittance for $(80-x)B_2O_3-xBi_2O_3-10P_2O_5-10ZnO$ glasses: (a) $x = 40$ mol%; (b) $x = 45$ mol%; (c) appearance of the glass samples.

and 8(b), it can be found that the decreasing trend of T_g and T_d of the glass with added Sb_2O_3 is smoother than that of the glass without added Sb_2O_3; and this phenomenon in 1,100°C molten glass ($+0Sb_2O_3$), as shown in Figure 9(a), also has the same trend, even after the addition of $3Sb_2O_3$, as shown in Figure 9(b). T_g, T_d hardly change with the increase of Bi_2O_3 content. This phenomenon is also confirmed by the results of the Raman glass structure analysis, as shown in the Raman analyses of Figures 1 and 2; with the addition of Sb_2O_3 to the glass, the peak change trend at 135 cm^{-1} with the increase in the content of Bi_2O_3 is more moderate compared with that of the glass without Sb_2O_3 added, this shows that the increase in the number of Bi–O–Bi bonds is relatively small, and the decreasing trend of the strength of the glass structure is also relatively small. Therefore, after the addition of Sb_2O_3, the trend of change in T_g and T_d is relatively small. $CTE = 7.7 \times 10^{-6}$/°C (Bi_2O_3 30 mol%), $CTE = 9.0 \times 10^{-6}$/°C (Bi_2O_3 35 mol%), $CTE = 9.17 \times 10^{-6}$/°C ($Bi_2O_3$ 40 mol%), CTE increases with increasing Bi_2O_3 content and the structural strength of the glass tends to decrease with Bi_2O_3 content.

3.3.2. Physical Properties of Glass. The density of glass is related to the mass of the atoms of the oxides that make up the glass and is the most important factor affecting the density of glass. In addition, the stacking and coordination of the atoms in the glass structure also affect the density of the glass. The molar volume of glass is obtained by dividing the molecular weight of the glass constituent oxides by the density. From the formula, it can be seen that the density of glass is inversely proportional to the molar volume, so usually, the molar volume of glass decreases as the density increases.

Figures 10 and 11 show the effect of composition on density and Molar volume for $(80-x)B_2O_3-xBi_2O_3-10P_2O_5-10ZnO + (0, 3Sb_2O_3)$ melted at 1,000 and 1,100°C.

Figure 10(a) is a graph of the relationship between the composition of the original glass and the influence of the composition on the density and molar volume of the glass melted at 1,000°C, and it can be seen from the figure that when the content of Bi_2O_3 increases, the density increases from 5.0 to 6.1 g/cm^3, and the molar volume increases from 39.39 to 42.03 cm^3/mol.

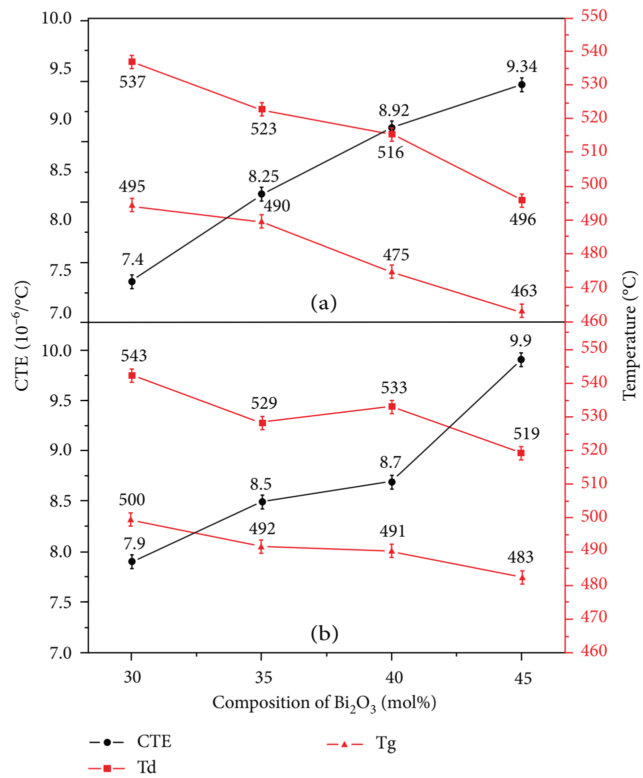

FIGURE 8: Thermal analysis of glass melted at 1,000°C: (a) $(80-x)B_2O_3$–xBi_2O_3–$10P_2O_5$–10ZnO; (b) $(80-x)B_2O_3$–xBi_2O_3–$10P_2O_5$–10ZnO + $3Sb_2O_3$.

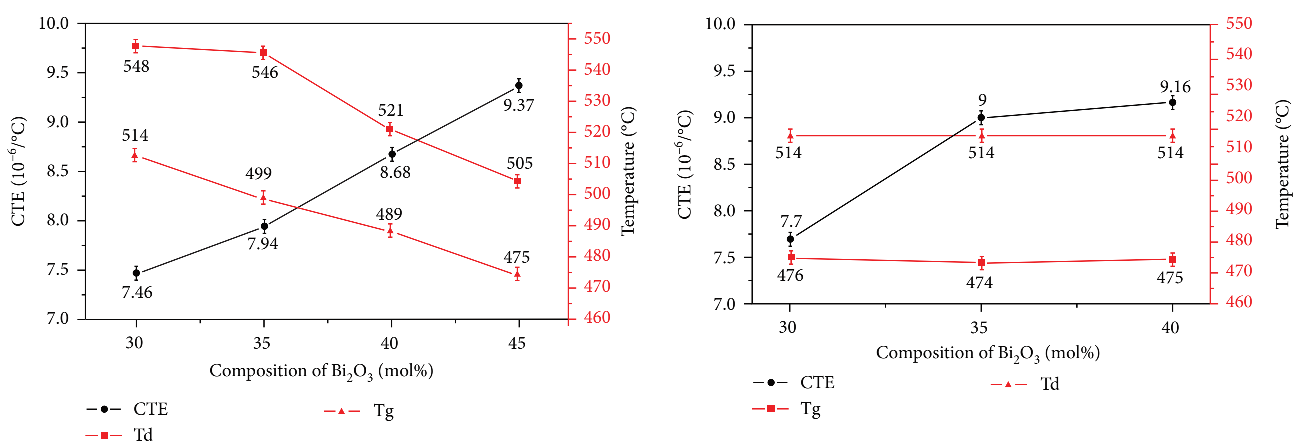

(a) (b)

FIGURE 9: Thermal analysis of glass melted at 1,100°C: (a) $(80-x)B_2O_3$–xBi_2O_3–$10P_2O_5$–10ZnO; (b) $(80-x)B_2O_3$–xBi_2O_3–$10P_2O_5$–10ZnO + $3Sb_2O_3$.

Figure 10(b) is the relationship diagram of the influence of the composition on the density and the molar volume of the glass melted at 1,000°C with the original glass composition + $3Sb_2O_3$, and it can be seen from the figure that when the content of Bi_2O_3 increases, the density increases from 5.18 to 6.2 g/cm^3, and the molar volume increases from 39.71 to 42.76 cm^3/mol.

Figure 11(a) shows the effect of composition on density and molar volume for the glass with the original glass composition melted at 1,100°C, and it can be observed that as the Bi_2O_3 content increases, so does the density and molar volume of the glass, with the density increasing from 4.91 to 5.93 g/cm^3 and the molar volume increasing from 40.10 to 43.23 cm^3/mol.

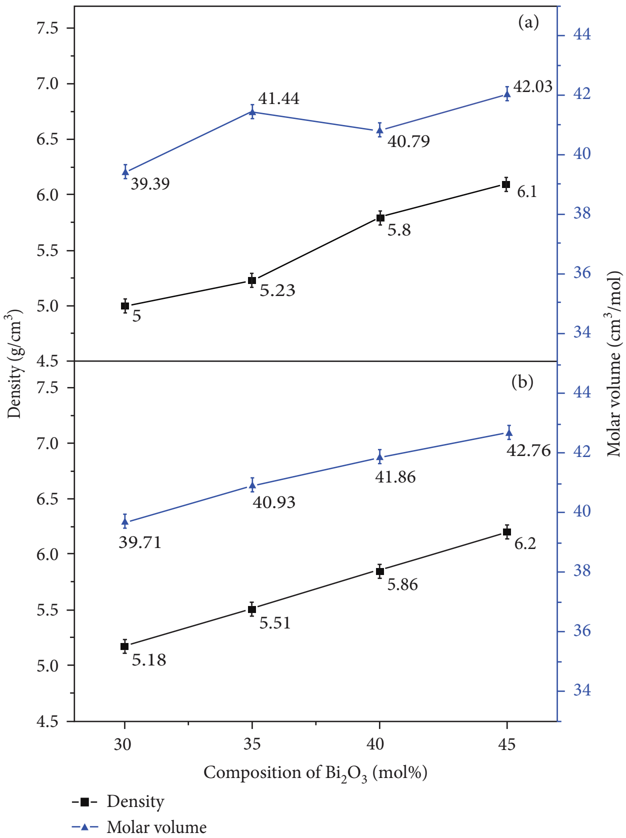

FIGURE 10: (a) $(80-x)B_2O_3$–xBi_2O_3–$10P_2O_5$–10ZnO; (b) $(80-x)B_2O_3$–xBi_2O_3–$10P_2O_5$–10ZnO + $3Sb_2O_3$ melted at 1,000°C as a function of glass composition and density and molar volume diagram.

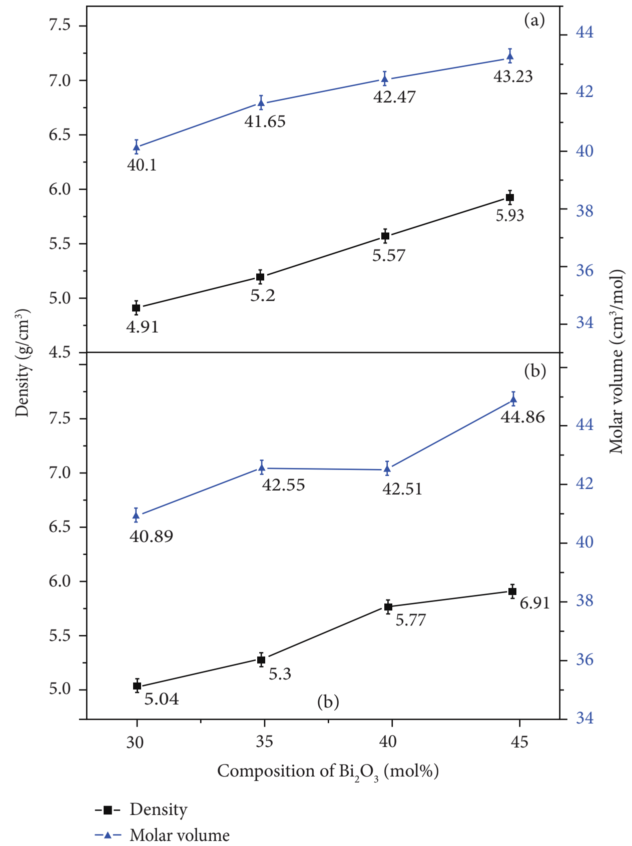

FIGURE 11: (a) $(80-x)B_2O_3$–xBi_2O_3–$10P_2O_5$–10ZnO; (b) $(80-x)B_2O_3$–xBi_2O_3–$10P_2O_5$–10ZnO + $3Sb_2O_3$ melted at 1,100°C as a function of glass composition and density and molar volume diagram.

Figure 11(b) shows the effect of composition on density and molar volume for the original glass composition and the addition of $3Sb_2O_3$ melted at 1,100°C, and the graph shows that the density increases from 5.04 to 5.91 g/cm^3 and the molar volume increases from 40.89 to 44.86 cm^3/mol as the Bi_2O_3 content increases.

The density of glass of all compositions, with or without the addition of Sb_2O_3, tends to increase as the Bi_2O_3 content increases; the main reason is that the atomic weight of Bi (208.98 g/mol) is much larger than that of B (10.81 g/mol), so when Bi_2O_3 replaces some of the boron atoms, the density increases. However, the formula for calculating the molar volume shows that the molar volume is inversely proportional to the density, but in all glasses, as the content of Bi_2O_3 increases, the molar volume and density both show an increasing trend; this is because the atomic weight of Bi is much larger than that of other glass constituent atoms. When calculating the molar volume, the rate of increase of atomic weight is greater than that of density, and the radius (1.2 Å) of Bi ions is also larger than that of other ions, thus increasing the free volume of the glass as a whole. In addition, the results of Raman structure analysis can also be found, the characteristic peak of the NBO of the (BiO_6) unit at wavenumber 570 cm^{-1}, as shown in Figures 1 and 2, increases slightly with increasing Bi_2O_3 content, indicating that the structure of the glass in this system has become more open due to the increased amount of NBO, resulting in an increase in the mole volume of the glass.

4. Conclusion

(1) In the $(80-x)B_2O_3$–xBi_2O_3–$10P_2O_5$–10ZnO series of glasses, the color of the glass melted at 1,100°C without the addition of Sb_2O_3 deepens with the increase in Bi_2O_3 content and melting temperature, while the addition of Sb_2O_3 significantly improves the transparency.

(2) From Raman analysis, this series of glasses has (BiO_3), (BiO_6), (BO_3), and (BO_4) structural units. As the Bi_2O_3 content increases from 30 to 45 mol%, the number of Bi–O–Bi and B–O–Bi bonds increases, and after the addition of Sb_2O_3, the number of these Bi–O–Bi bonds is relatively small.

(3) In the UV–Vis transmittance spectrum, the cutoff wavelength shifted to a longer wavelength as the Bi_2O_3 content increased from 30 to 45 mol%. With the increase in melt temperature to 1,100°C, Bi^0 was produced, resulting in a significant decrease in transmittance and an orange-brown appearance with an absorption peak at about 470 nm.

(4) As the Bi_2O_3 content increases from 30 to 45 mol %, the density and Molar volume of the glass show an increasing trend.

(5) With the increase of Bi_2O_3 content from 30 to 45 mol%, the glass transition temperature (T_g) and glass softening temperature (T_d) of this series of glasses decreased, while the CTE increased, which is consistent with the increase in the number of Bi–O–Bi and B–O–Bi bonding in Raman results. In this study, it was found that the color of the glass appearance changed from black to light yellow when comparing the main ingredient (no added Sb_2O_3) with a small amount of added Sb_2O_3; the decolorization effect is significant. These glasses have the potential to low-temperature optical molding applications.

Data Availability

The data of Raman spectra, transmittance curves, thermal analysis, density, and molar volume used to support the findings of this study are included within the article.

Conflicts of Interest

The authors declare that there is no conflict of interest regarding the publication of this paper.

Acknowledgments

The authors gratefully acknowledge the financial support of the Ministry of Science and Technology (MOST), Taipei, Taiwan, R.O.C. and the National Sci-Tech Programs: The study on manufacture and sealing characterization of bismuth–zinc borate glasses (MOST 103-2221-E-239-005).

References

[1] F. He, J. Wang, and D. Deng, "Effect of Bi_2O_3 on structure and wetting studies of Bi_2O_3–ZnO–B_2O_3 glasses," *Journal of Alloys and Compounds*, vol. 509, no. 21, pp. 6332–6336, 2011.

[2] E. Haily, L. Bih, M. Jerroudi, M. Azrour, A. El bouari, and B. Manoun, "Structural investigation of SrO–BaO–TiO_2–B_2O_3–P_2O_5 glass–ceramics," *Materials Today: Proceedings*, vol. 37, Part 3, pp. 3798–3802, 2021.

[3] E. Haily, L. Bih, A. El Bouari, A. Lahmar, M. El Marssi, and B. Manoun, "Structural, optical, and dielectric properties of Bi_2O_3–K_2O–TiO_2–P_2O_5 glasses and related," *Phase Transitions*, vol. 93, no. 10-11, pp. 1030–1047, 2020.

[4] E. Haily, L. Bih, A. El Bouari, A. Lahmar, M. El Marssi, and B. Manoun, "Effect of the Ba/K ratio on structural, dielectric and energy storage properties of BaO–K_2O–TiO_2–P_2O_5 glass–ceramics," *Physics and Chemistry of Glasses-European Journal of Glass Science and Technology Part B*, vol. 61, no. 6, pp. 213–221, 2020.

[5] E. Haily, L. Bih, A. El Bouari, A. Lahmar, M. El Marssi, and B. Manoun, "Structural, optical, and dielectric properties of the BaO–TiO_2–P_2O_5 glasses," *Journal of the Australian Ceramic Society*, vol. 56, pp. 1467–1479, 2020.

[6] E. Haily, L. Bih, A. El bouari, A. Lahmar, M. Elmarssi, and B. Manoun, "Effect of BaO–Bi_2O_3–P_2O_5 glass additive on structural, dielectric and energy storage properties of $BaTiO_3$ ceramics," *Materials Chemistry and Physics*, vol. 241, Article ID 122434, 2020.

[7] E. Haily, L. Bih, M. Jerroudi, S. Yousfi, A. El bouari, and B. Manoun, "Structural and dielectric properties of K_2O–TiO_2–P_2O_5 glass and its associated glass–ceramic," *Materials Today: Proceedings*, vol. 30, Part 4, pp. 849–853, 2020.

[8] M. Hrovat, T. Maeder, J. Holc, D. Belavič, J. Cilenšek, and J. Bernard, "Subsolidus phase equilibria in the RuO_2–Bi_2O_3–SiO_2 system," *Journal of The European Ceramic Society*, vol. 28, pp. 2221–2224, 2008.

[9] S. P. Singh and B. Karmakar, "Bismuth oxide and bismuth oxide doped glasses for optical and photonic applications," *Materials Chemistry and Physics*, vol. 119, pp. 355–358, 2010.

[10] G. Gao, L. Hu, H. Fan et al., "Effect of Bi_2O_3 on physical, optical and structural properties of boron silicon bismuthate glasses," *Optical Materials*, vol. 32, no. 1, pp. 159–163, 2009.

[11] Y. Zhang, Y. Yang, Y. Ou, W. Hua, J. Zheng, and G. Chen, "Effect of Sb_2O_3 on thermal properties of glasses in Bi_2O_3–B_2O_3–SiO_2 system," *Journal of the American Ceramic Society*, vol. 92, no. 8, pp. 1881–1883, 2009.

[12] S.-H. Lan, C.-T. Lee, Y.-S. Lai, C.-C. Chen, and H.-W. Yang, "The relationship between the structure and thermal properties of Bi_2O_3–ZnO–B_2O_3 glass system," *Advances in Condensed Matter Physics*, vol. 2021, Article ID 2321558, 12 pages, 2021.

[13] W.-X. Wang and H.-W. Yang, *The Study on The Decolorization and Properties of Bismuth Glass*, National United University, Taiwan, R.O.C, 2020, https://hdl.handle.net/11296/78x25r.

[14] L. Baia, R. Stefan, J. Popp, S. Simon, and W. Kiefer, "Vibrational spectroscopy of highly iron doped B_2O_3–Bi_2O_3 glass systems," *Journal of Non-Crystalline Solids*, vol. 324, no. 1-2, pp. 109–117, 2003.

[15] L. Baia, R. Stefan, W. Kiefer, J. Popp, and S. Simon, "Structural investigations of copper doped B_2O_3–Bi_2O_3 glasses with high bismuth oxide content," *Journal of Non-Crystalline Solids*, vol. 303, no. 3, pp. 379–386, 2002.

[16] L. Baia, R. Stefan, W. Kiefer, and S. Simon, "Structural characteristics of B_2O_3–Bi_2O_3 glasses with high transition metal oxide content," *Journal of Raman Spectroscopy*, vol. 36, no. 3, pp. 262–266, 2005.

[17] M. Abdel-Baki, F. A. Abdel-Wahab, A. Radi, and F. El-Diasty, "Factors affecting optical dispersion in borate glass systems," *Journal of Physics and Chemistry of Solids*, vol. 68, no. 8, pp. 1457–1470, 2007.

[18] Y. D. Yiannopoulos, G. D. Chryssikos, and E. I. Kamitsos, "Structure and properties of alkaline earth borate glasses," *Physics and Chemistry of Glasses*, vol. 42, no. 3, pp. 164–172, 2001.

[19] S. Bale, N. S. Rao, and S. Rahman, "Spectroscopic studies of Bi_2O_3–Li_2O–ZnO–B_2O_3 glasses," *Solid State Sciences*, vol. 10, no. 3, pp. 326–331, 2008.

[20] Z. Pan, D. O. Henderson, and S. H. Morgan, "Vibrational spectra of bismuth silicate glasses and hydrogen-induced reduction effects," *Journal of Non-Crystalline Solids*, vol. 171, no. 2, pp. 134–140, 1994.

[21] B. N. Meera and J. Ramakrishna, "Raman spectral studies of borate glasses," *Journal of Non-Crystalline Solids*, vol. 159, no. 1-2, pp. 1–21, 1993.

[22] B. N. Meera, A. K. Sood, N. Chandrabhas, and J. Ramakrishna, "Raman study of lead borate glasses," *Journal of Non-Crystalline Solids*, vol. 126, no. 3, pp. 224–230, 1990.

[23] G. D. Chryssikos, M. S. Bitsis, J. A. Kapoutsis, and E. I. Kamitsos, “Vibrational investigation of lithium metaborate-metaaluminate glasses and crystals,” *Journal of Non-Crystalline Solids*, vol. 217, no. 2-3, pp. 278–290, 1997.

[24] S. Bale, S. Rahmana, A. M. Awasthi, and V. Sathe, “Role of Bi_2O_3 content on physical, optical and vibrational studies in Bi_2O_3–ZnO–B_2O_3 glasses,” *Journal of Alloys and Compounds*, vol. 460, no. 1-2, pp. 699–703, 2008.

[25] Y. B. Saddeek and M. S. Gaafar, “Physical and structural properties of some bismuth borate glasses,” *Materials Chemistry and Physics*, vol. 115, no. 1, pp. 280–286, 2009.

[26] A. A. Kharlamov, R. M. Almeida, and J. Heo, “Vibrational spectra and structure of heavy metal oxide glasses,” *Journal of Non-Crystalline Solids*, vol. 202, no. 3, pp. 233–240, 1996.

[27] J. E. Shelby, *Introduction to Glass Science and Technology*, Royal Society of Chemistry, 2005.

[28] E. Haily, L. Bih, M. Jerroudi, and A. El bouari, “Optical properties and frequency-dependent conductivity of K_2O–BaO–TiO_2–P_2O_5 glasses,” *Materials Today: Proceedings*, vol. 51, Part 6, pp. 2027–2031, 2022.